# Elastic prestack migration of two component data

*John T. Etgen*


## ABSTRACT

P and SV waves recorded with two component geophones can be migrated before stack to form images of the subsurface. If the source contains only P waves, the recorded wave field (for land data) will contain both P and SV waves. If the data are separated into P and SV potentials, separate migration equations can be written, one for P–P reflections and one for P–SV reflections (mode conversions). Separate migration of P and SV waves may have some advantages over fully coupled P–SV migration. Separate P–P and P–SV wave migrations allow for more inaccuracy in the velocity model than fully coupled migration. Some care must be given to the imaging condition to avoid problems with polarity reversals of the SV potential across zero offset. When the data are collected on a regular grid, a version of Stolt's $\omega, k_h, k_m$ migration technique can be applied. When the shot sampling is not uniform, it may be advantageous to migrate individual shot profiles and stack the results. For the Stolt algorithm, a P–P wave velocity space and a P–SV wave velocity space can be built allowing the estimation of P and SV wave velocities from the migrated images.


## INTRODUCTION

Although the earth is more closely approximated by a linear elastic medium than an acoustic medium, exploration geophysicists have long ignored the elastic behavior of wave propagation. As it becomes more important to extract as much information from seismic data as possible, the importance of using elastic wave propagation in modeling and processing increases.

Recently several authors have proposed methods to migrate or invert elastic wave fields before stack (Mora, 1987), ( Tarantola, 1982), (Chang and McMechan, 1987), (Kuo and Dai, 1984). To date, the most common approaches to elastic migration use the coupled elastic wave equation for wave extrapolation. This paper takes a different tack. I will separate P and SV wave potentials from the elastic wave field recorded on two component geophones and migrate these wave potentials separately to form multiple images of the subsurface. If the source excites only P waves, two images can be obtained, a P–P image (similar to conventional processing) and a P–SV image. If the source contained only SV waves, both an SV–SV image and a SV–P image are obtained.

Propagating the P and SV wave potentials separately may have advantages compared to extrapolating the coupled, two-component elastic wave field. When migrating elastic wave fields using the coupled elastic wave equation, the imaging conditions usually require that the P and SV waves coalesce at the reflector simultaneously to be imaged properly. If either the P or SV velocity is not known well, the P and SV waves will not image at the same depth; this will degrade the images. Anisotropy often affects SV waves to a greater degree than P waves, so it will be quite possible that the P and SV waves will not image at the same depth unless the coupled extrapolation is anisotropic and the horizontal and vertical velocities are known. If P and SV wave potentials are extrapolated and imaged separately, the SV wave velocity and P wave velocity are used separately; velocity error can be tolerated. Each image can be examined independently, or compared with the other. This should make it easier to find the effects of anisotropy or velocity error.

## Migration of P–P and P–SV waves

Prestack migration of elastic waves is very similar to prestack migration of acoustic waves. I present two methods for migrating elastic wave fields after separating the up-coming elastic wave field into P and SV potentials.

### Imaging conditions

Chang and McMechan (1987) presented a method for elastic migration that used coupled reverse-time extrapolation of the two-component elastic wave field. The imaging condition they presented was purely kinematic; the travel time of the source wave field was obtained by ray tracing. Imaging at a given point is accomplished by selecting the value of the wave field at the one way travel time from the source. Using a purely kinematic imaging condition will not always be satisfactory, because elastic wave fields can have complicated amplitude distributions which will not be unraveled if the imaging operator only uses traveltimes.

Claerbout (1985) formalized the concept of imaging up and down-going waves for acoustic media. The same ideas can be applied to elastic migration. Reflectors are found by deconvolving (or in practice cross correlating) the up and down-going wave fields. If P and SV waves are separated, the extension from the acoustic case is straightforward. Rather than simply correlating down-going P waves with up-coming P waves (as in the acoustic case), both P and SV up-coming waves are correlated with the down-going P wave field in the case of a P wave source. If the

P and SV waves have complicated radiation patterns, this imaging condition will be better than a purely kinematic imaging operator.

### Separating P and SV waves

If the velocity of the subsurface is not known, it is wise to migrate P and SV wave reflections from a P wave source separately. Coupled extrapolation requires both P and SV waves to image simultaneously; if the P wave velocity is known but the SV wave velocity is not, the image will be degraded. If the P and SV waves are downward continued and imaged separately, the P wave image will not be distorted by the incorrect SV wave image. Furthermore, it is possible to tell that the SV wave velocity was incorrect and the P wave velocity was correct. P waves can be extracted from a two-component elastic wave field by applying the divergence operator to the wave field vector. SV waves can be extracted by applying the curl operator to the wave field vector.

$$P = \nabla \cdot \mathbf{U} \ ; \ SV = \nabla \times \mathbf{U}$$

$$P = \frac{\partial U_x}{\partial x} + \frac{\partial U_z}{\partial z} \ ; \ SV = \frac{\partial U_z}{\partial x} - \frac{\partial U_x}{\partial z} \tag{1}$$

Oristaglio et al. (1985), presented a Fourier domain implementation of wave separation based on divergence and curl applied to P and SV wave separation in a borehole. In the Fourier domain, the P wave potential can be determined by applying the Fourier transform of the divergence operator to the elastic wave field to annihilate the SV waves.

$$P(\omega, k_x) = ik_x U_x(\omega, k_x) - i\sqrt{\omega^2/\beta^2 - k_x^2}\,U_z(\omega, k_x) \quad . \tag{2}$$

The SV wave potential can be determined by applying the Fourier transform of the curl operator to annihilate P waves.

$$SV(\omega, k_x) = ik_x U_z(\omega, k_x) + i\sqrt{\omega^2/\alpha^2 - k_x^2}\,U_x(\omega, k_x) \quad . \tag{3}$$

The P wave velocity is $\alpha$ and the SV wave velocity is $\beta$. This method is only exact when the surface velocity of P and SV waves, $\alpha$ and $\beta$ respectively, are independent of $x$. Oristaglio et al., showed that the method works well even when the velocity does vary along transformed direction. For surface seismic data excited by an explosive source, the SV potential changes sign across zero offset. To get the correct sign of the reflectivity, the negative offsets must be multiplied by -1 or an imaging condition based on displacements must be used.

### Phase shift shot profile migration

The phase shift method (Gazdag, 1978) can be applied to both the P wave potential as well as the SV wave potential to downward continue the wave field recorded at the surface. Upcoming SV waves can be extrapolated in depth by applying the phase shift factor $exp(ik_z\Delta z)$ to the Fourier transform of the SV wave potential. For SV waves, $k_z$ is has the form

$$k_z = -\frac{\omega}{\beta}\sqrt{1 - \frac{\beta^2 k_x^2}{\omega^2}} \quad . \tag{4}$$

When $k_x$ exceeds $\omega/\beta$, $k_z$ is chosen to be positive imaginary. This ensures evanescent energy decays with depth. $k_z$ has the opposite sign as $\omega$ to downward extrapolate up-coming waves. Apply the phase shift factor to the SV potential at level $z$ to downward continue it to level $z + \Delta z$.

$$SV(\omega, k_x, z + \Delta z) = SV(\omega, k_x, z) exp(ik_z\Delta z) \tag{5}$$

Upcoming P waves can also be extrapolated in depth by applying the phase shift factor $exp(ik_z\Delta z)$ to the Fourier transform of the P wave potential. For P waves, $k_z$ is has the form

$$k_z = -\frac{\omega}{\alpha}\sqrt{1 - \frac{\alpha^2 k_x^2}{\omega^2}} \quad . \tag{6}$$

When $k_x$ exceeds $\omega/\alpha$, $k_z$ is again chosen to be positive imaginary. The same convention is taken for up-coming waves as above. The P potential at each $z$ level is found by applying the phase shift to the data from the previous level.

$$P(\omega, k_x, z + \Delta z) = P(\omega, k_x, z) exp(ik_z\Delta z) \tag{7}$$

If the P and SV wave potentials were obtained from a shot profile, the shot profile can be migrated by specifying a down-going source wave field. If we assume the source excited only P waves, the source wave field can be downward continued by applying the phase shift factor $exp(ik_z\Delta z)$ where $k_z$ is given by

$$k_z = \frac{\omega}{\alpha}\sqrt{1 - \frac{\alpha^2 k_x^2}{\omega^2}} \quad . \tag{8}$$

For down-going waves, $k_z$ has the same sign as $\omega$ for downward continuation. The source wave field at each $z$ level is found by phase shifting the source wave field from the previous level.

$$P_s(\omega, k_x, z + \Delta z) = P_s(\omega, k_x, z) exp(ik_z\Delta z) \tag{9}$$

Imaging the P–P reflectivity is accomplished by inverse transforming up and down-going waves in $x$ and taking the zero lag of the time correlation of the up and down-going P waves at each depth.

$$R_{PP}(x, z) = \sum_{\omega} P(\omega, x, z) P_s^*(\omega, x, z) \ , \tag{10}$$

where $*$ denotes complex conjugation. In a similar fashion, the P–SV reflectivity is found by inverse transforming up and down-going waves in $x$ and taking the zero lag of the time correlation of the up-coming SV wave field and the down-going P wave field at each depth.

$$R_{PSV}(x,z) = \sum_{\omega} SV(\omega,x,z)P_s^*(\omega,x,z) \tag{11}$$

The phase shift method is only exact when velocity does not vary in the $x$ direction. When velocity varies laterally, a thin lens term can be applied to correct the downward continued wave fields approximately for lateral velocity variation (Claerbout, 1985). This approach is also known as the "Split-step Fourier Method" (Freire and Stoffa, 1986). The thin lens term is a phase shift in the $x, \omega$ domain.

$$thinlens(x) = exp\Big[i\omega(\frac{1}{v_{avg}(z)} - \frac{1}{v(x,z)})\Big] \ . \tag{12}$$

To incorporate this into the downward continuation and imaging scheme, for each extrapolation step in depth, apply the standard phase shift (equation 5 or 7) in the $k_x, \omega$ domain, inverse transform to $x, \omega$, and apply the thin lens term.

$$F'(\omega,k_x,z+\Delta z) = F(\omega,k_x,z)exp(ik_z\Delta z)$$

$$F'(\omega,x,z+\Delta z) = FT_x^{-1}\Big[F'(\omega,k_x,z+\Delta z)\Big]$$

$$F(\omega,x,z+\Delta z) = F'(\omega,x,z+\Delta z)exp\Big[i\omega(\frac{1}{v_{avg}(z)} - \frac{1}{v(x,z)})\Big] \ . \tag{13}$$

where $F$ is either the P or SV wave potential and $v$ is either $\alpha$ or $\beta$ respectively. $v_{avg}(z)$ is the velocity used for downward continuation; $v(x,z)$ is the true laterally varying velocity. For the next depth step, the wave fields must be Fourier transformed back to $k_x, \omega$. The thin lens term for down-going waves is the conjugate of the thin lens term above.

## Stolt $\omega$, $k_h$, $k_m$ migration

In a constant velocity medium, prestack migration can be accomplished by a Stolt change of variables in the Fourier domain followed by inverse transformation (Stolt, 1978). I will derive prestack Stolt migration for P–SV reflectivity, and review the P–P case as well. As for phase shift migration, the first step of processing the elastic wave field is the separation of the two-component data in up-coming P and SV potentials. the SV wave potential has a sign change for negative offsets which can be corrected by multiplying all negative offset traces of the SV wave potential after separation by $-1$. The up-coming P wave and SV wave potentials can be sorted into midpoint–offset coordinates and 3-D Fourier transformed. The dispersion relation for up-coming P waves due to a P wave source is

$$k_{z_P} = \frac{\omega}{\alpha}\sqrt{1 - \frac{\alpha^2 k_s^2}{\omega^2}} + \frac{\omega}{\alpha}\sqrt{1 - \frac{\alpha^2 k_g^2}{\omega^2}} \ . \tag{14}$$

The dispersion relation for up-coming SV waves due to a P wave source is

$$k_{z_{SV}} = \frac{\omega}{\alpha}\sqrt{1 - \frac{\alpha^2 k_s^2}{\omega^2}} + \frac{\omega}{\beta}\sqrt{1 - \frac{\beta^2 k_g^2}{\omega^2}} \ . \tag{15}$$

In either case, we have the choice of working in midpoint–offset coordinates or in shot–geophone coordinates. There is a simple relation between $k_s$, $k_g$, and $k_h$, $k_m$.

$$k_s = \frac{k_m - k_h}{2} \ ; \ k_g = \frac{k_m + k_h}{2}$$

We can take an expression using shot and geophone wavenumbers and translate it to use midpoint–offset wavenumbers. For the P–P reflectivity migration is accomplished by downward continuing by multiplication by $exp(ik_{z_P} z)$, imaging at $t = 0$, $h = 0$, changing variables from $\omega$ to $k_{z_P}$ and inverse transforming to midpoint and depth. Likewise, migration of P–SV reflected waves is accomplished by multiplication by $exp(ik_{z_{SV}})$, imaging at $t = 0$, $h = 0$, changing variables from $\omega$ to $k_{z_{SV}}$ and inverse transformation to midpoint and depth. Write the downward continued wave potentials as

$$P(k_m, k_h, w, z) = P(k_m, k_h, w, z = 0) exp(ik_{z_P} z) \ . \tag{16}$$

$$SV(k_m, k_h, w, z) = SV(k_m, k_h, w, z = 0) exp(ik_{z_{SV}} z) \ . \tag{17}$$

Evaluating at $t = 0$, $h = 0$ images the P–P or P–SV reflectivity.

$$R_{PP}(k_m, z) = \int dk_h \int dw \ P(k_m, k_h, w) exp(ik_{z_P} z) \ . \tag{18}$$

$$R_{PSV}(k_m, z) = \int dk_h \int dw \ SV(k_m, k_h, w) exp(ik_{z_{SV}} z) \ . \tag{19}$$

Now make the change of variables from $\omega$ to $k_z$ in each inner integral

$$R_{PP}(k_m, z) = \int dk_h \int dk_{z_P} \left| \frac{d\omega}{dk_{z_P}} \right| P(k_m, k_h, w(k_{z_P})) exp(ik_{z_P} z) \ . \tag{20}$$

$$R_{PSV}(k_m, z) = \int dk_h \int dk_{z_{SV}} \left| \frac{d\omega}{dk_{z_{SV}}} \right| SV(k_m, k_h, w(k_{z_{SV}})) exp(ik_{z_{SV}} z) \ . \tag{21}$$

In practice, the change of variables is a regridding of the $\omega$ axis to the $k_z$ axis by interpolation of the known values. The regridding requires the evaluation of $\omega$ as a function of $k_z$. For P–P migration, $\omega(k_z)$ can be written as

$$\omega(k_m, k_h, k_{z_P}) = \frac{\alpha k_z}{2}\sqrt{(1 + \frac{(k_g + k_s)^2}{k_z^2})(1 + \frac{(k_g - k_s)^2}{k_z^2})} \ . \tag{22}$$

For P–SV migration $\omega(k_z)$ is slightly more complicated than the P–P expression, but can be written in the form

$$\omega(k_m, k_h, k_{z_{SV}}) =$$

$$\sqrt{\frac{Ak_z^2 + B(k_s^2 - k_g^2) - 2\alpha^2\beta^2\sqrt{\alpha^2\beta^2k_z^4 + k_z^2(k_s^2(\alpha^2\beta^2 - \alpha^4) + k_g^2(\alpha^2\beta^2 - \beta^4))}}{\beta^4 - 2\alpha^2\beta^2 + \alpha^4}} \quad , \tag{23}$$

where

$$A = \alpha^4\beta^2 + \beta^4\alpha^2 \ ; \ B = \alpha^2\beta^4 - \alpha^4\beta^2 \quad .$$

The expression of the Jacobian $|\frac{d\omega}{dk_z}|$ for the P–P wave case can be found in Van Trier (1986). For the P–SV case the Jacobian can be found in Appendix A of this paper. The appropriate expression in midpoint–offset coordinates can be found by plugging in the relations between $k_s$, $k_g$ and $k_m$, $k_h$. After regridding the $\omega$ axis to $k_z$ for each $k_h$ and $k_m$, the results are summed over $k_h$ and inverse transformed to midpoint and depth obtaining the migrated P–P or P–SV reflectivity image.

It is possible to compute the image of P–P wave reflections in a variable velocity medium by computing constant velocity images with prestack Stolt migration for a range of velocities and interpolating the variable velocity image from the image cube (Fowler, 1985). The same approach could be applied to P–SV reflections. Apply the Stolt migration algorithm derived above to the up-coming SV wave potential for a range of P and SV velocities. If P and SV velocities are scanned independently, a 4-dimensional velocity space results. Rather than scan through both P and SV wave velocities independently, it makes sense to scan through P wave velocities and several different values of $\alpha/\beta$, the P to S wave velocity ratio. Although this space is also 4-dimensional the number of values of $\alpha/\beta$ should be less than if all SV wave velocities were considered independently ( Dellinger, pers. comm.). Once a P wave root-mean-square velocity curve is known, those values of the 4-dimensional P–SV velocity space can be extracted from each cube of constant $\alpha/\beta$, reducing the volume to 3 dimensions. The peaks of the stack power in this space will estimate $\alpha_{rms}/\beta_{rms}$ with midpoint and depth. This should prove to be a valuable velocity analysis tool for converted wave reflections, as it has for P–P wave data.

## EXAMPLES

To test the migration algorithms, a synthetic data set was modeled using an elastic finite-difference modeling program. Figure 1 shows the horizontal and vertical components of particle displacement for 1 shot profile. The free surface was replaced by an absorbing surface so no Rayleigh waves are present. This also simplified wave type separation, because only up-coming waves will be present at the receivers. For real data, a more sophisticated wave separation method is needed. An explosive source (P waves only) was used for each shot record. The migration programs of this paper use the separated P and SV potentials, so the two component shot records were separated into the two wave potentials. Figure 2 shows one shot record separated into P and SV potentials. To avoid the change of sign of the SV

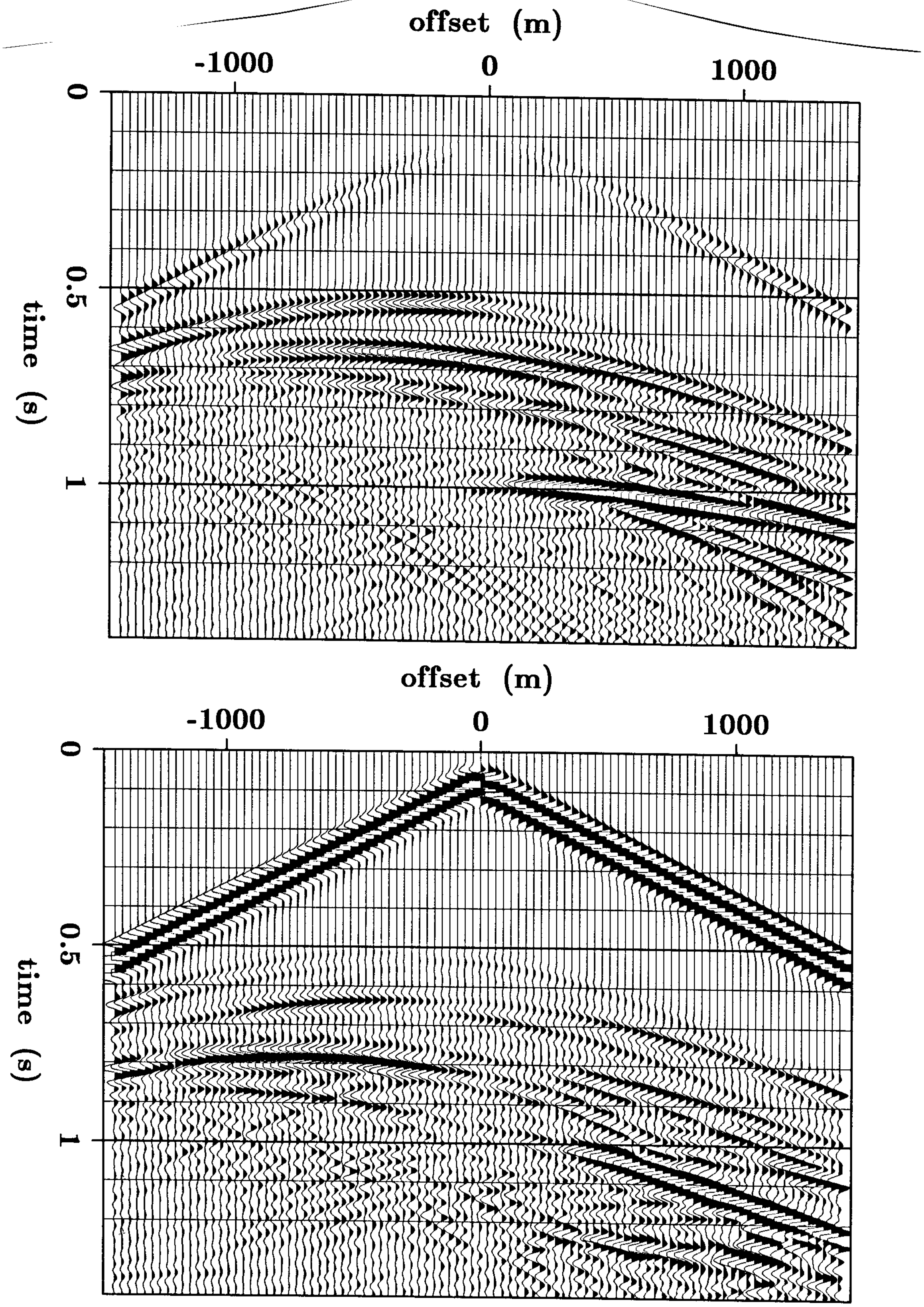


FIG. 1. Two-component shot record used as input to elastic migration techniques. The top gather is the vertical component shot record, the bottom gather is the inline horizontal shot record.

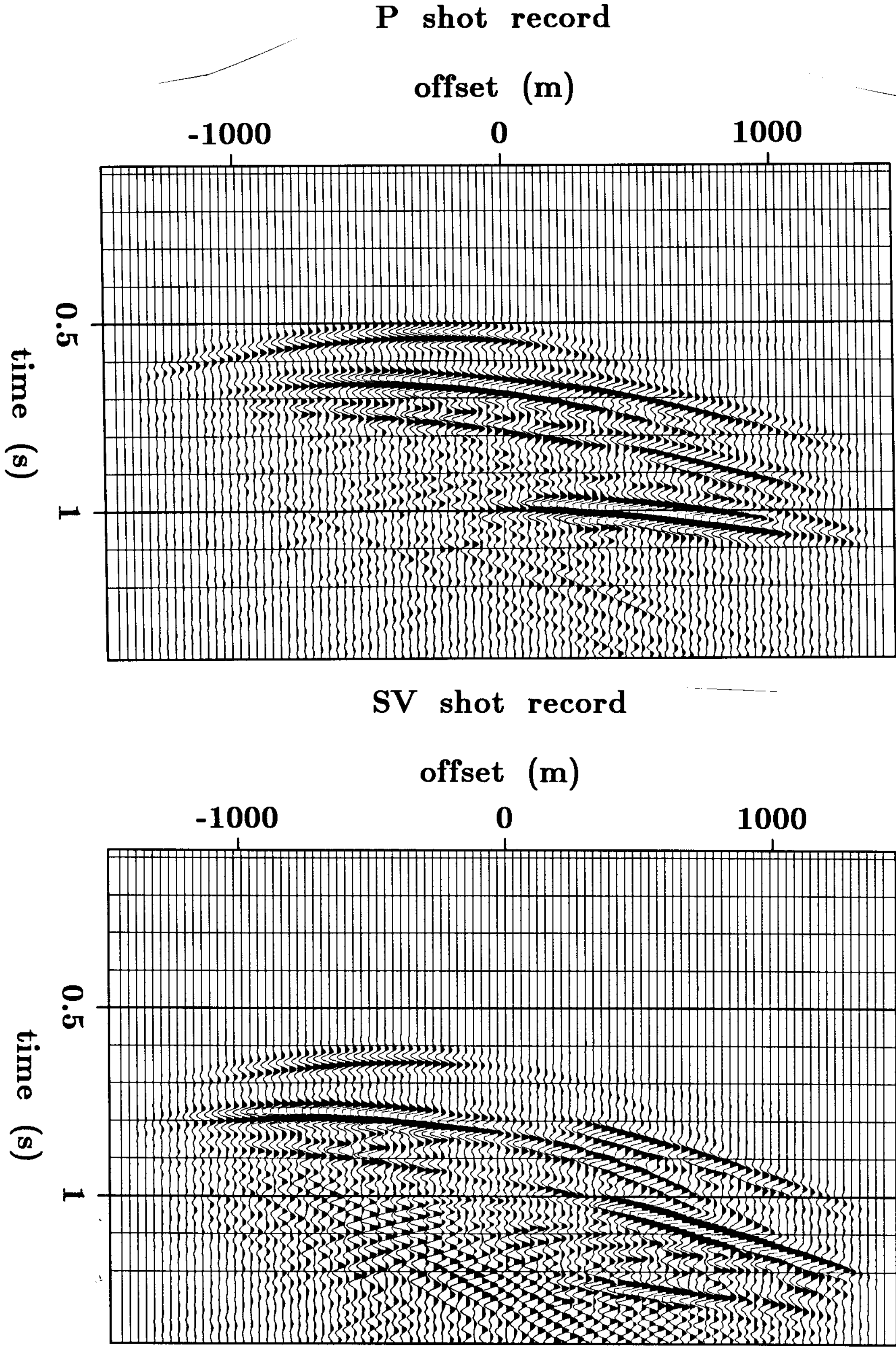


FIG. 2. Shot record separated into up-coming P and SV waves. P waves are on the top and SV waves are on the bottom. The data has been gained by multiplying by $t$ and the direct waves muted.

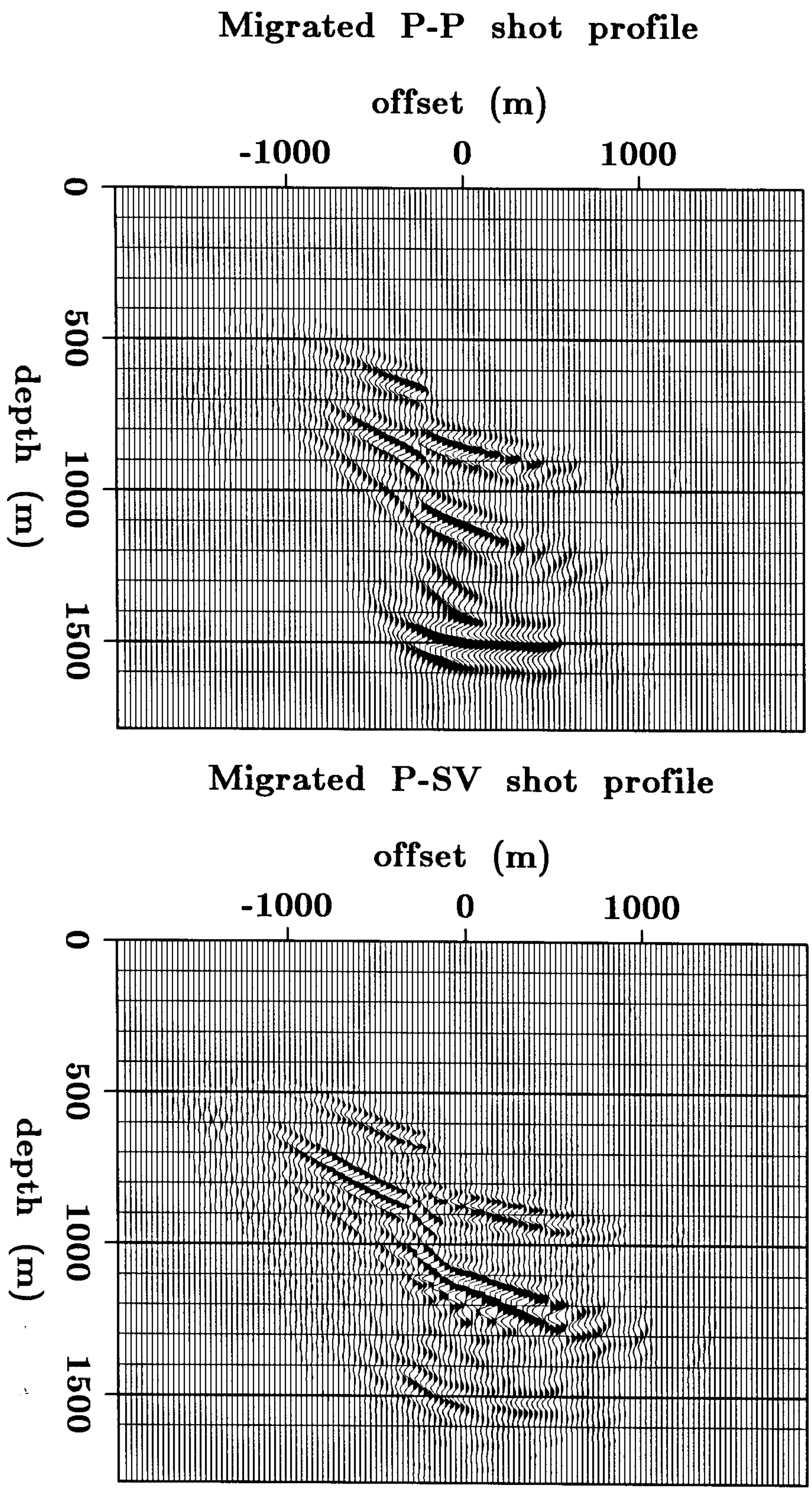


FIG. 3. Migrated P–P shot record and migrated P–SV shot record.

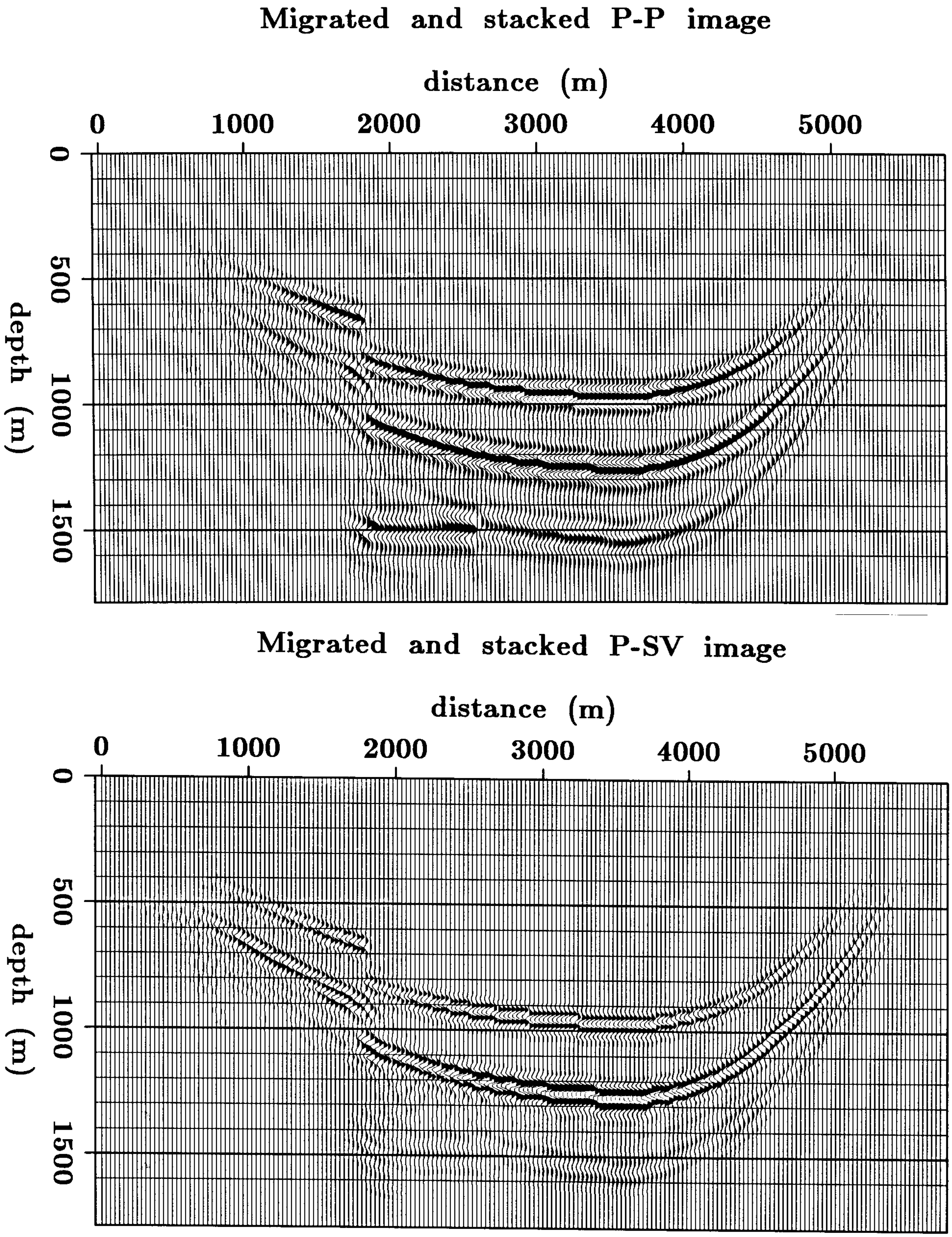


FIG. 4. The stack of 64 migrated P–P shot records is at the top and the stack of 64 migrated P–SV shot records is at the bottom. The phase shift method has successfully migrated both the P–P reflections and the P–SV reflections.

potential, the negative offsets of the SV potential shot record must be multiplied by $-1$. The phase shift shot record migration program was applied to each separated shot gather. Both P and SV waves were downward continued and imaged with a down-going P wave source wave field. Figure 3 shows the resulting P–P and P–SV images for one shot record. In each case, the images of the reflectors can be seen. Figure 4 shows the stack of 64 migrated P and SV wave shot profiles.

The same 64 shot profiles were sorted into midpoint-offset coordinates after separation, and 3-D Fourier transformed. The Stolt migration method was applied to the P wave data for a range of P wave velocities, and the SV wave data was imaged at a range of P wave velocities and a range of P to S wave velocity ratios, $\alpha/\beta$. Figure 5 shows a constant offset section of the P wave and SV wave data. Figure 6 shows the image of the P–P wave data for two velocities. Figure 7 shows the image of the SV wave data for two constant P wave velocities for $\alpha/\beta = 1.50$, which is close to the true value in the model. Figure 8 shows one midpoint of the P wave image and one midpoint of the SV wave image for several different P wave velocities; $\alpha/\beta$ is fixed at 1.50. Figure 9 shows the one midpoint of the migrated SV wave image for all values of $\alpha$ and 3 values of $\alpha/\beta$. If a greater range of P wave velocities and $\alpha/\beta$ were included, the velocity analysis property of this display would be more obvious.

## CONCLUSIONS

If P and SV waves are separated from the elastic wave field recorded with two-component geophones, simple prestack migration algorithms can be designed that do not require solving the coupled elastic wave equation. These migration algorithms are similar to the prestack migration algorithms used on acoustic wave data. Using separate extrapolation for P and S waves should make velocity analysis of converted waves easier. Some care must be taken with imaging conditions because SV waves have a sign change across zero offset.

## REFERENCES

Chang, W. F., and McMechan, G. A., 1987, Elastic reverse-time migration: Geophysics, **52**, 1365–1375.

Claerbout, J. F., 1985, Imaging the Earth's interior: Blackwell Scientific Publications, London.

Freire, R., and Stoffa, P. L., 1986, Migration using the "split-step" Fourier method: Presented at the 56th Annual International SEG meeting in Houston.

Gazdag, J., 1978, Wave-equation migration with the phase shift method: Geophysics, **43**, 1342–1351.

Kuo, J. T., and Dai, T. F., 1984, Kirchhoff elastic wave migration for the case of noncoincident source and receiver: Geophysics, **49**, 1223-1238.

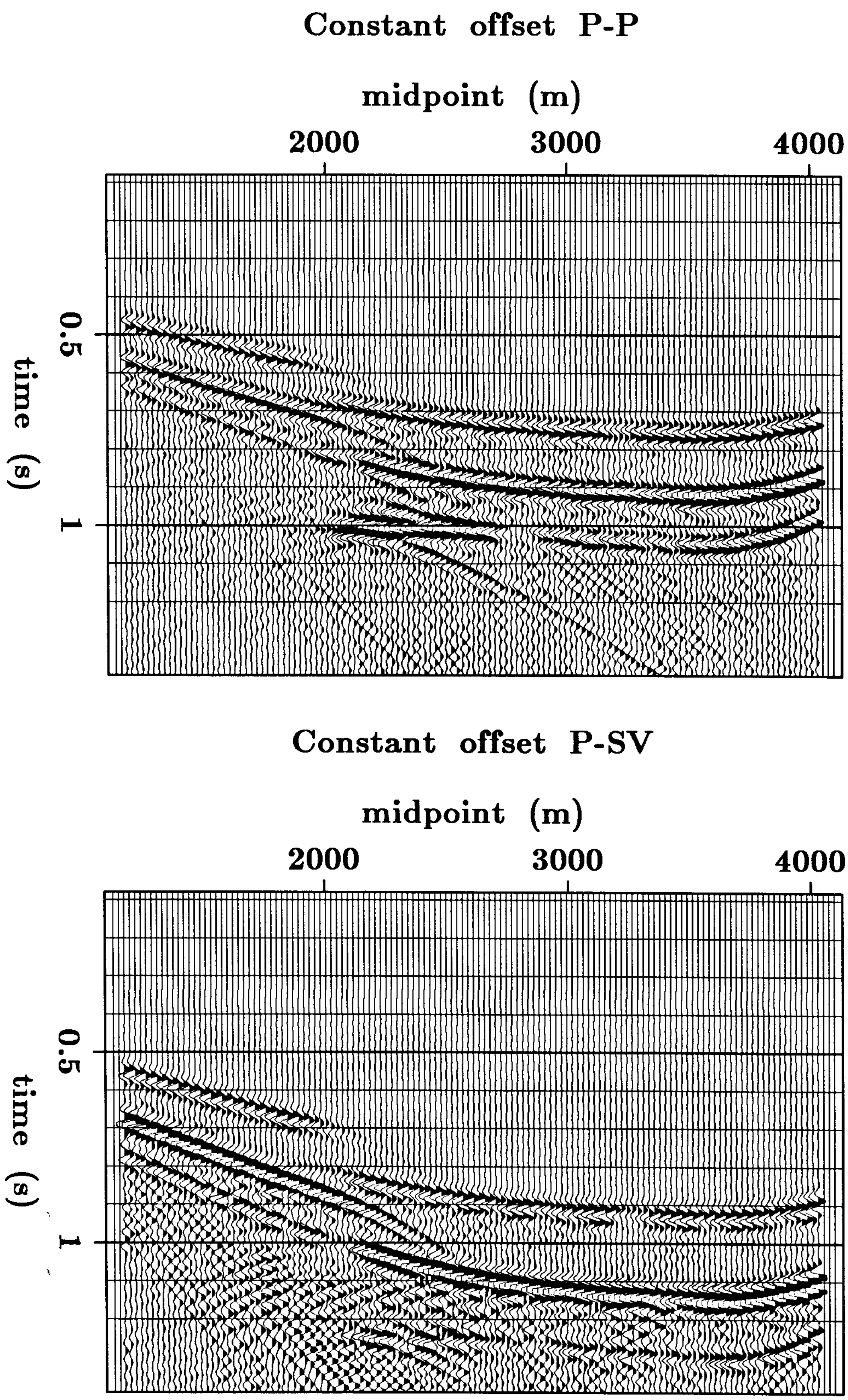


FIG. 5. Constant offset sections of the P wave and SV wave potentials before prestack migration.

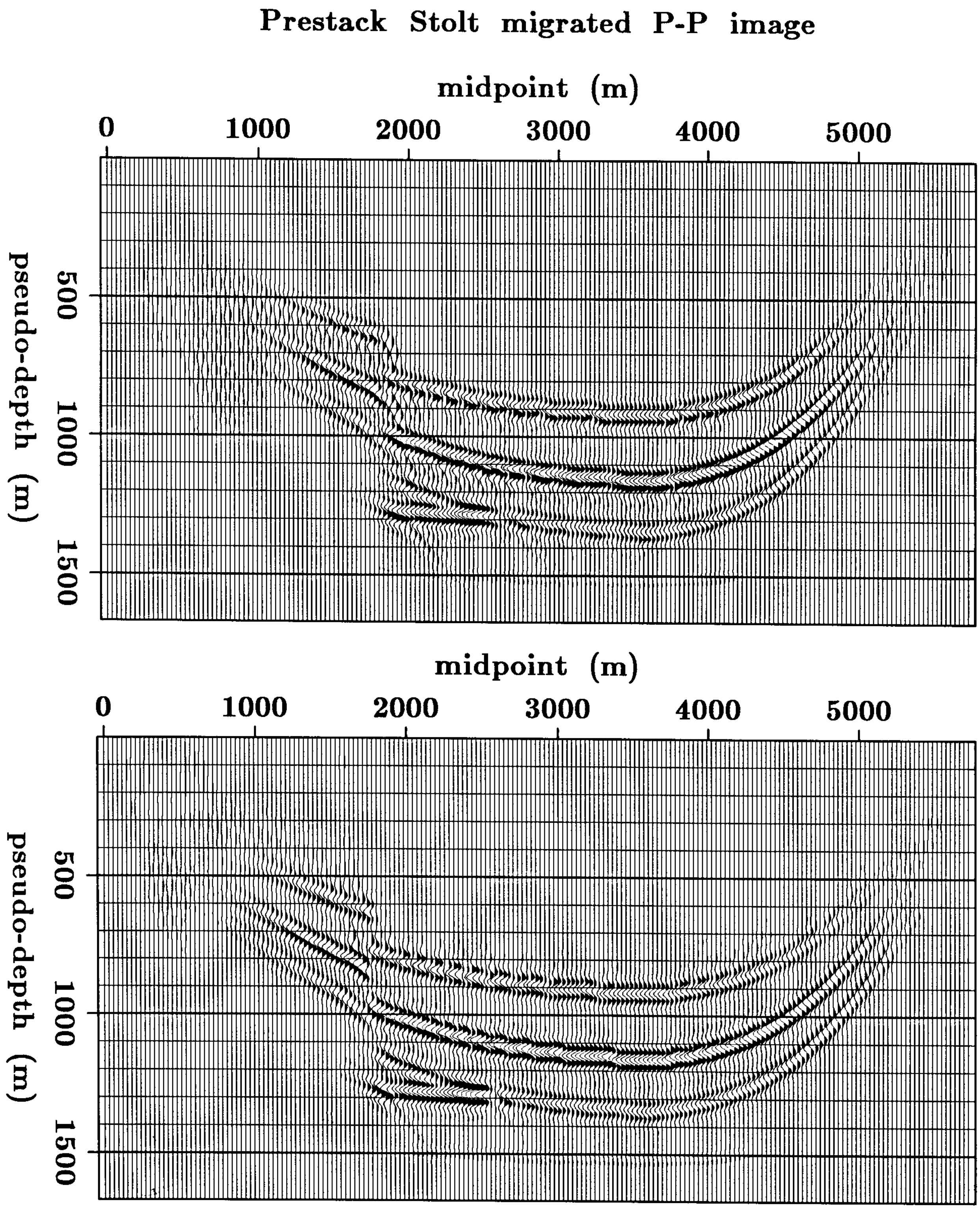


FIG. 6. Migrated image of P–P reflectivity using prestack Stolt migration. Since the velocity used for migration in each panel is constant, not all reflectors are perfectly focused in one panel. A well focused image could be obtained by extracting the image of each reflector from the panel at the velocity that best focuses the event.

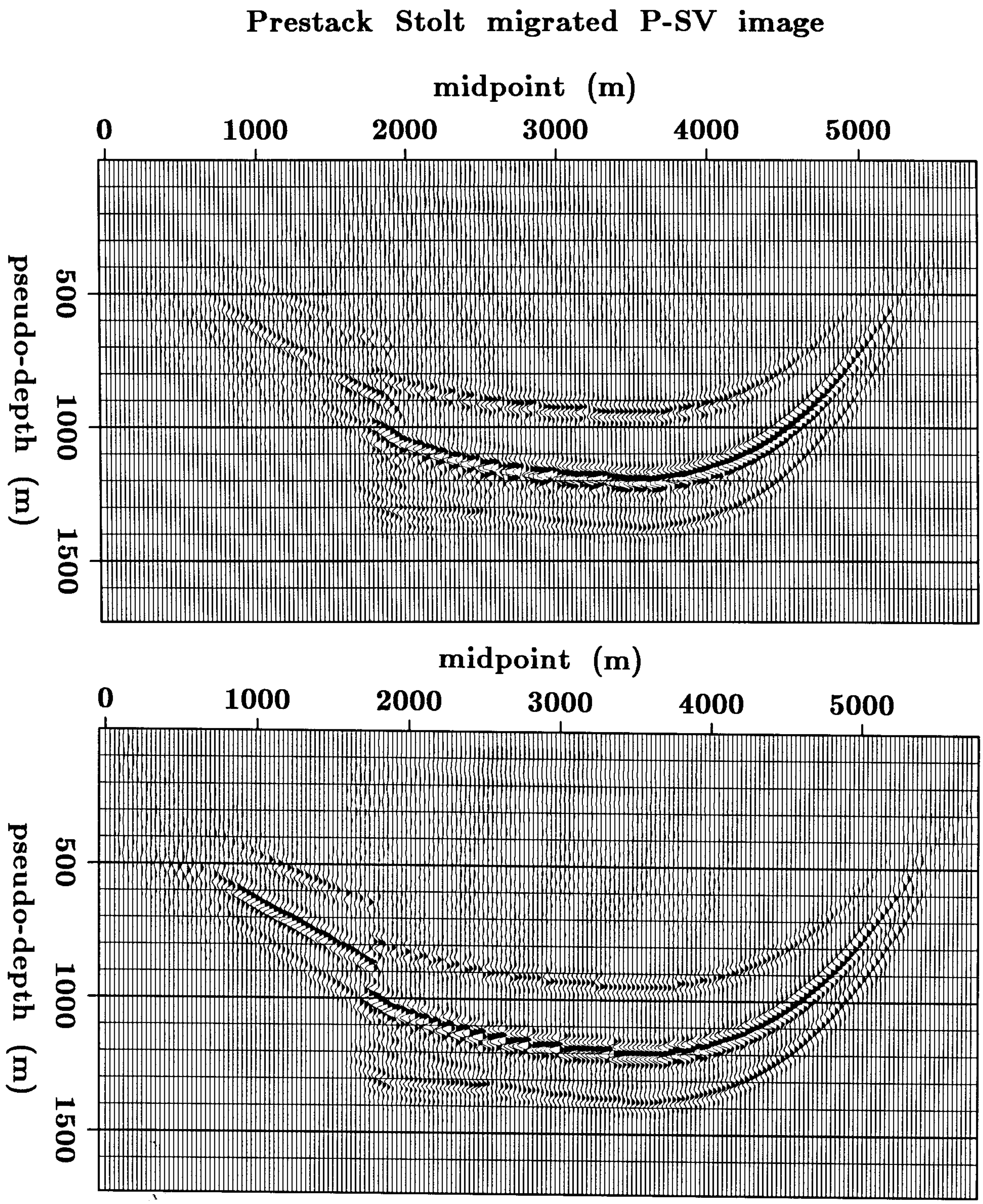


FIG. 7. Migrated image of P–SV reflectivity using prestack Stolt migration at two P wave velocities for one value of the P to S wave velocity ratio. Since the velocity used for migration in each panel is constant, not all reflectors are perfectly focused in one panel. A well focused image could be obtained by extracting the image of each reflector from the panel at the velocity that best focuses the event.

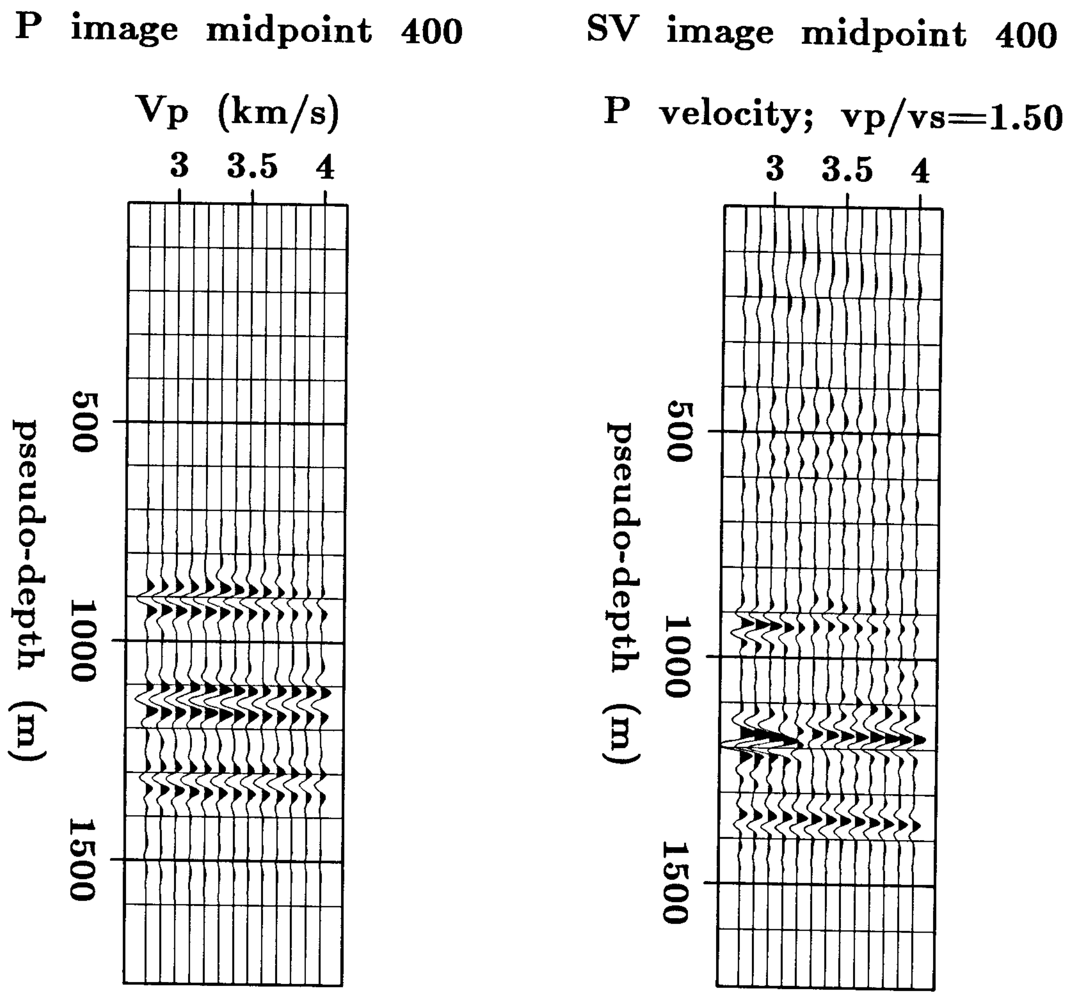


FIG. 8. Migrated image of one midpoint using prestack Stolt migration of the P–P and P–SV waves for a range of P wave velocities and fixed P to S wave velocity ratio. Velocity analysis for P waves can be performed by finding the migration velocities that best focus the events.

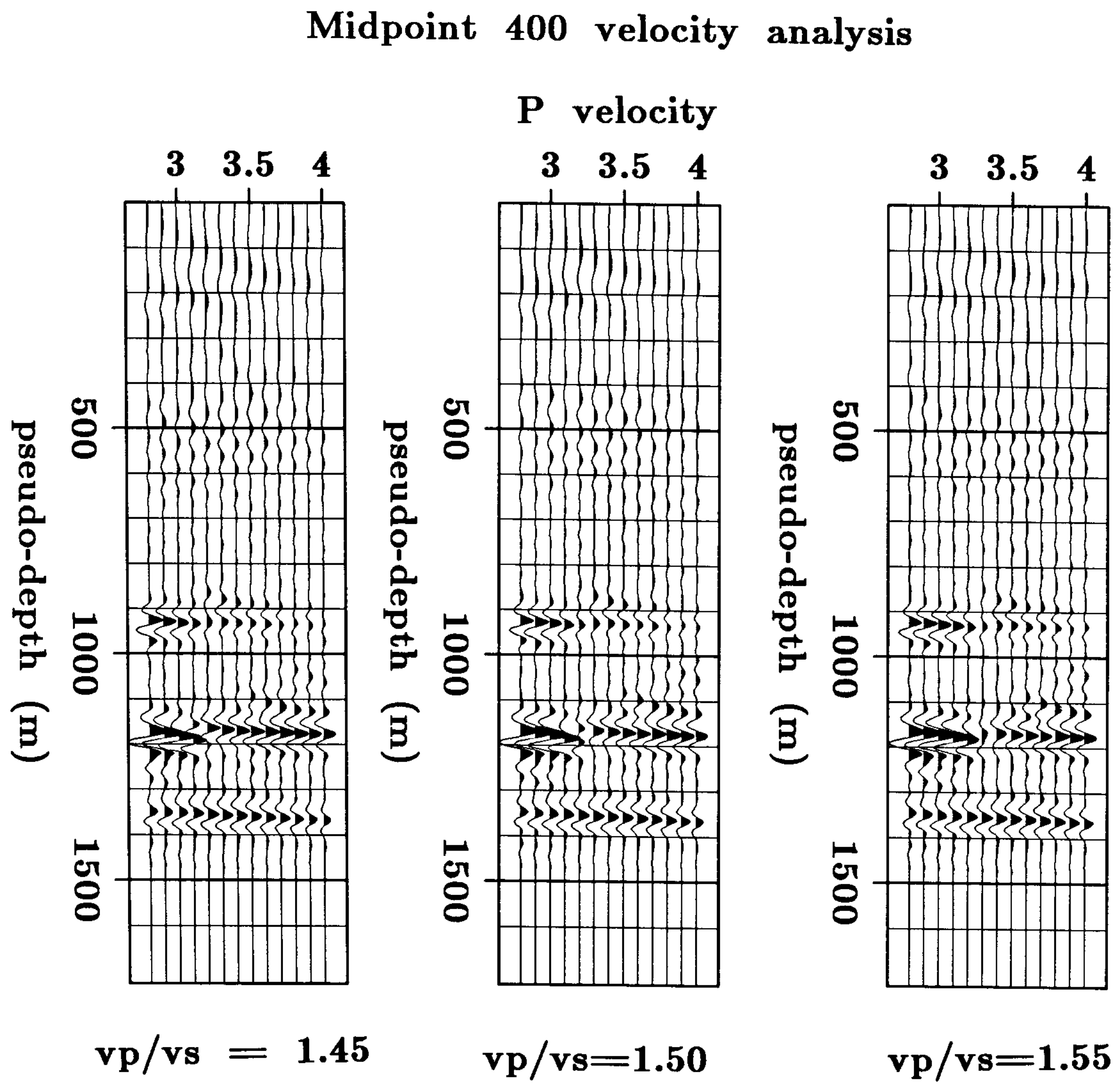


FIG. 9. Migrated image of one midpoint of the P–SV wave data for several values of the P to S wave velocity ratio and all P wave velocities used for migration. The space of all midpoints and all P wave velocities and P to S wave velocity ratios is a converted wave velocity space that can be used for velocity analysis.

Mora, P., 1986, Nonlinear 2d elastic inversion of multi-offset seismic data: SEP–**48**, 167–226.

Oristaglio, M. L., Devany, A. J., and Track, A., 1985, Separation of P-waves and S-waves in borehole seismic data: Presented at the 55th Annual International SEG meeting in Washington D.C.

Tarantola A., and Valette, B., 1982, Inverse problems = quest for information: Journal of geophysics, **50**, 159–170.

Stolt, R. H., 1978, Migration by Fourier transform: Geophysics, **43**, 23–48.

Van Trier, J., 1986, Inversion of seismic data in the Fourier domain and prestack Stolt migration: SEP–**48**, 227–242.

## APPENDIX A

The Jacobian of the change of variables from $k_{z_{SV}}$ to $\omega$ can be derived as follows. Take equation 23 of the text and differentiate with respect to $k_z$.

$$\frac{d\omega}{dk_z} = \frac{1}{2(\beta^4 - 2\alpha^2\beta^2 + \alpha^4)} \frac{1}{\omega(k_z)}$$

$$\left[2k_z(\alpha^4\beta^2 + \alpha^2\beta^4) - \alpha^2\beta^2 \frac{4\alpha^2\beta^2 k_z^3 + 2k_z(k_s^2(\alpha^2\beta^2 - \alpha^4) + k_g^2(\alpha^2\beta^2 - \beta^4))}{\sqrt{\alpha^2\beta^2 k_z^4 + k_z^2(k_s^2(\alpha^2\beta^2 - \alpha^4) + k_g^2(\alpha^2\beta^2 - \beta^4))}}\right] . \quad (A.1)$$

$\left|\frac{d\omega}{dk_z}\right|$ is just the absolute value of the above expression.